ACCOUNTS
of chemical research

Area-Selective Growth of Functional Molecular Architectures

WENCHONG WANG AND LIFENG CHI*

Physikalisches Institut and Center for Nanotechnology (CeNTech), Universität Münster, 48149 Münster, Germany

RECEIVED ON NOVEMBER 30, 2011

CONSPECTUS

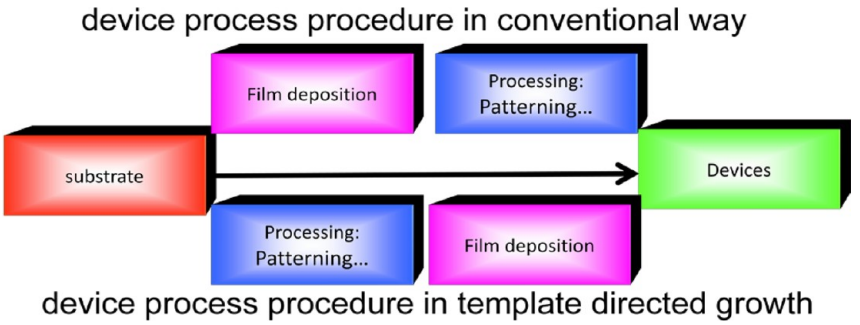

Over the last two decades, organic semiconductors have attracted increasing attention because of the applications of their inorganic counterparts in a growing number of devices. At the same time, the further success of these materials will require device processing techniques for organic semiconductors that produce high performance and high integration over large areas. Conventional top-down patterning techniques based on photolithography have served powerful methods for the surface patterning of inorganic materials. However, researchers cannot simply transfer these techniques to organic semiconductors because organic semiconductors can include small, fragile organic molecules. Alternatively, researchers have developed several nonconventional techniques, including shadow mask, printing, and vapor jet writing. However, no leading technique has emerged, and researchers are still trying to realize batch-to-batch, and even device-to-device, reproducibility.

This Account summarizes recent research in our group aimed at developing methods for patterning small organic molecules that are compatible with standard device processing procedures for inorganic semiconductors. Our concept is based on classic growth dynamics by gas-phase deposition but leads to different selective growth mechanisms: "pre-patterning and patterned growth" instead of the traditional "film growth and patterning." As a result, both "foreign body" and "step edge", two possible nucleation positions for atoms and molecules during thin film growth process, can be enlarged to the mesotropic scale to define molecules within pre-determined areas.

The techniques can do more than patterning. We demonstrate that these techniques can produce heteropatterning of organic structures that cannot be obtained by conventional photolithography and printing techniques. Through a combination of different growth modes, we can separate molecules at given locations on the mesotropic scale, which could lead to applications in the production of organic solar cells. Taking advantage of the differences in emission of molecules in different aggregation states, we can achieve tunable single, double- and triple-color patterns using two types of molecules. We also show that these materials can lead to devices with improved performance in features such as carrier mobility.

In addition, we believe that this new photographic compatible procedure in small molecular organic semiconductors can address some issues in device performance, such as carrier transport in organic field effect transistors, by controlling domain size and numbers, and allow researchers to explore new nanoscale properties of these materials. The techniques are still in their infancy, and further research is needed to make them applicable, such as transferring the technology to cheap substrates, for example, glass and flexible plastic. For organic electronics, high-level integration, addressable, and cross-talk free device arrays are critical for producing high-performance devices at a low fabrication cost.

Introduction

Functional, small molecular weight organic molecules have received great scientific and technological interest due to their promising potential applications in molecular electronics and optoelectronics.[1−3] Over the last two decades, exciting progress has been witnessed in both material

Published on the Web 07/25/2012 www.pubs.acs.org/accounts
10.1021/ar200299w

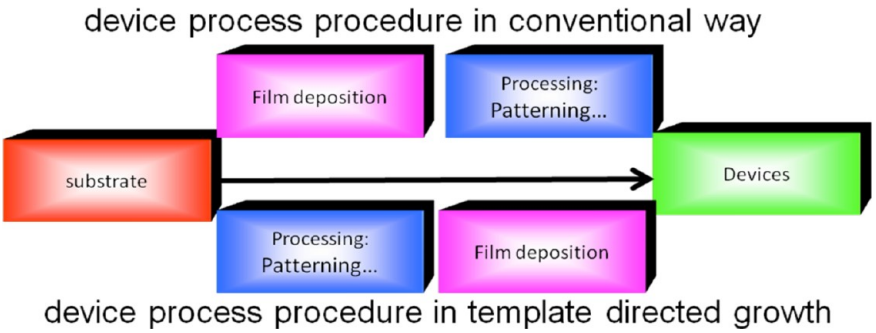

FIGURE 1. Schematic of device processing procedures in conventional way and template directed growth.

synthesis and film preparation that were applied for organic devices such as organic field effect transistors (OFETs),[4−8] light-emitting diodes (OLEDs),[9,10] solar cells,[11] memories,[12] sensors,[13] and so on. However, device processing techniques, patterning in particular, yielding high performances, high levels of integration, and uniformity over large area are still underdevelopment, because conventional top-down patterning techniques based on photolithography cannot be simply applied to organic systems.[14] Alternatively, techniques based on shadow masks,[15] subtractive printing,[16] additive printing,[17] vapor jet writing,[18] and even dewetting of liquid electrodes[19] have been developed. These techniques, however, suffer variously from insufficient resolution, poor scalability, and complicated multistep processing. A number of researchers have sought to develop photolithographic procedures by encapsulation of organic materials into metal or photoresist layers.[20,21] However, the procedures still have clear limitations, for example, involving a large number of processing steps.

A bottom-up strategy based on self-assembly provides another approach to generate structures with scale down possibilities even to the molecular level.[22] One of the major challenges for the application of these methods in electronics is addressing the structures by external circuits. The top-down assisted bottom-up (or template-directed assembly) strategy opens up a possible way to overcome the problems by defining the objects at predefined locations.[23] The technique provides control over structure, size, and morphology of various materials by using chemical templates, either by adsorption/desorption[7,24] or by diffusion/binding[25] processes. In 2007, we proposed a concept to pattern organic structures in gas-phase deposition on prepatterned surfaces.[26] In this Account, we will summarize our work on this topic since then, mainly based on the site-selective nucleation control on a prepatterned surface followed by different growth modes. We will further demonstrate the versatility of the technique for heteropatterning, for molecule separation, for physical property tuning, and in fabricating devices with improved performances.

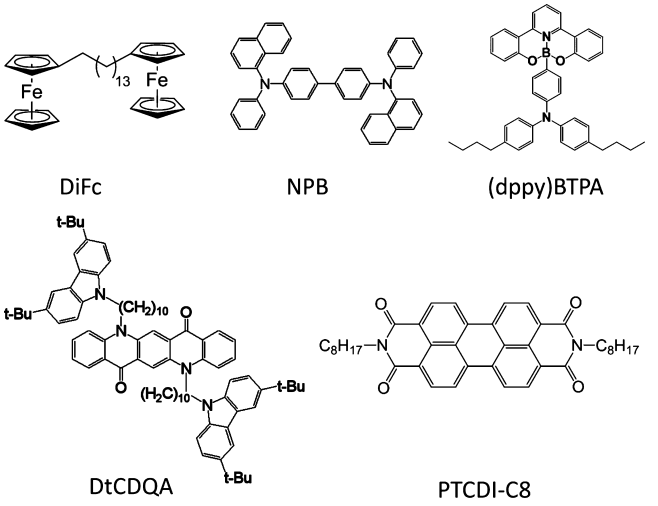

FIGURE 2. Chemical structures of the molecules used in the study.

Our basic motivation is illustrated in Figure 1. Instead of the procedure of film deposition on a substrate followed by device patterning, a typical device processing methodology usually applied to inorganic materials, we create the surface patterns first and then deposit molecules. By properly selection of molecules and optimization of prepattern dimensions (e.g., feature size, periodicity) and growth conditions (e.g., substrate temperature, growth rate), the molecules may diffuse over the substrate surface and nucleate on predefined locations and evolve to patterned structures and even to devices directly.

Template Induced Area-Selective Nucleation and Growth: The Basic Concept and Mechanisms

Molecules Used in This Study. Chemical structures of the molecules used in the studies are outlined in Figure 2. The diferrocene (DiFc) is a derivative of ferrocene containing two

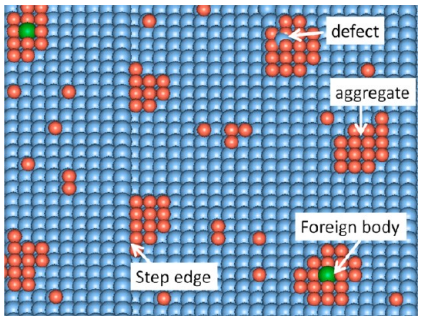

FIGURE 3. Molecule-scale view of growth process at a surface. Molecules are deposited from the vapor phase and diffuse over the substrate surface to form aggregates or nucleate at foreign bodies, defects, and step edges.

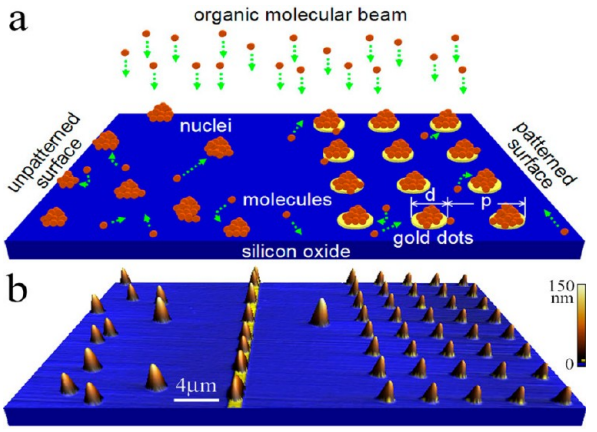

FIGURE 4. Template-directed nucleation control for organic molecule deposition: (a) schematic diagram; (b) AFM image of DiFc on partial Au dot patterned SiO_2 substrate. DiFc was deposited at a substrate temperature of 45 °C with a deposition rate of 0.1 nm/min. Adapted with permission from ref 26. Copyright 2007 American Physical Society.

ferrocenyl groups bridged by an oligoethylene chain.[27] The *N*,*N*′-bis-(1-naphyl)-*N*,*N*′-diphenyl-1,1′-biphenyl-4,4′-diamine (NPB) is a blue light-emitting, classic hole transport material widely used in high-performance OLEDs.[28] 1,6-Bis(2-hydroxyphenol)pyridinel boron bis(4-*n*-butyl-phenyl)-phenyleneamine ((dppy)BTPA) combines the light-emitting center with hole- and electron-transporting groups into one molecule, thus demonstrating a promising green/yellow light-emitting material.[29] *N*,*N*′-Di[(*N*-(3,6-di-*tert*-butyl-carbazyl))-*n*-decyl] quinacridone (DtCDQA) is an orange light-emitting material with high quantum yield.[30] *N*,*N*-Dioctyl-3,4,9,10-perylene tetracarboxylic diimide (PTCDI-C_8) is a typical n type organic semiconductor with electron mobility on the order of 1 $cm^2/(V \cdot s)$.[31]

Among the above-mentioned molecules, DiFc, NPB, DtCDQA, and (dppy)BTPA are nonplanar in configuration, which leads to weak van de Waals interaction when forming aggregates. AFM images of such molecules deposited on a bare SiO_2 surface show that the molecules aggregate together to form randomly distributed, dome-shaped islands.[26] In contrast, PTCDI-C_8 is a planar molecule with an extended π system. The molecules form layered films on a bare SiO_2 at optimized growth conditions owing to the strong $\pi-\pi$ interaction.[32]

Material growth from molecules by gas phase deposition is a nonequilibrium process governed by the competition between kinetics and thermodynamics. The basic growth process of molecules, which involves nucleation at energetically favorable sites to form islands and their temporal evolution, has been well characterized and found to closely mimic the epitaxial growth of inorganic materials.[33] In conventional nucleation theory, besides the aggregation, deposited atoms/molecules are thermally activated to diffuse on the surface preferably nucleating at defect sites,[34] step edges,[35] or foreign bodies[36] due to their relatively strong interaction to these specific locations, as schematically shown in Figure 3. The nuclei, which are not stable in the initial stage when the size is smaller than a critical value, will either disappear via desorption of molecules or grow to form the stable ones by capturing further molecules.[37] Position control of the molecular aggregation is usually difficult owing to untraceable diffusion trajectories. However, with pattern generating techniques, nucleation sites can be predesigned and created. In the following, we will demonstrate that lithography generated patterns can be used to provide nucleation centers, which can direct the growth of organic molecules and lead to organic molecule structures for patterning and device fabrication.

Area Selective Nucleation on Predefined Locations . Concept. Our concept for patterned growth of organic molecules by nucleation control is schematically illustrated in Figure 4a.[26] A substrate surface is prepatterned with materials with which the organic molecules have binding energies different from that with the substrate, for instance, Si/SiO_2 surface patterned with Au structures. On an unpatterned area, shown on left side of Figure 4a, a random distribution of nuclei is expected owing to random diffusion of the molecules over the surface. In contrast, on a prepatterned area shown on the right side of Figure 4a, the molecules may nucleate on the prepatterned positions for energy reasons if they are able to arrive there via surface diffusion. The idea was experimentally proven by using DiFc, which has a large diffusion length on Si/SiO_2 even at room temperature, as shown in Figure 4b with islands randomly distributed on the unpatterned surface (left part) and exclusively on predefined Au dots (right part).

Full Nucleation Control and Mechanism behind It. The realization of full nucleation control includes several key parameters. For a better description, we defined a nucleation control efficiency (NCE) as $x_{NCE} = N_{Au}/N$ and a characteristic length scale $\lambda = (N/A)^{-1/2}$, where N_{Au} and N are the number of Au dots and the total number of organic islands, respectively, and A is the surface area of the counted islands. In this way, λ is a measure for the distance between adjacent islands, which is dependent on the substrate surface, the type of molecules, the substrate temperature T, and the growth rate F. With λ, we introduce a dimensionless periodicity $p^* = p/\lambda$, where p is the periodicity of the prepatterned dot array. Having p^*, we can directly compare x_{NCE} of different experiments in the same graph, as shown in Figure 5, which contains DiFc and NPB grown on substrates with different T and p. As demonstrated in Figure 5, when λ is greater than p ($p^* < 1$), x_{NCE} equals unity, indicating the full control of nucleation on Au dots. On the other hand, when λ is smaller than p ($p^* > 1$), x_{NCE} decreases as p^* increases, indicating the partial control of nucleation. In general, for a given molecule and substrate surface, large diffusion length, resulting from high T and low F, and small p will help to achieve full NCE control.

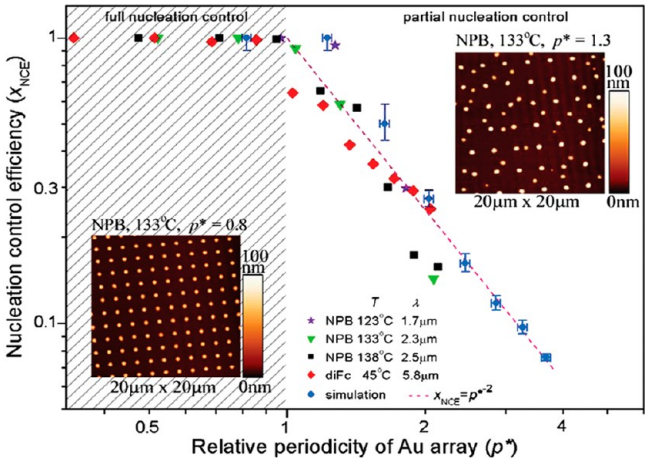

FIGURE 5. Relationship between the nucleation control efficiency (x_{NCE}) and the relative periodicity (p^*) obtained from experiments and MC simulations. When $p^* < 1$, x_{NCE} equals unity, indicating the full control of nucleation. When $p^* > 1$, x_{NCE} is gradually decreased, indicating partial control of nucleation. The dashed pink line shows the relationship $x_{NCE} = p^{*-2}$, which should hold for $x_{NCE} \ll 1$. Insets are AFM images of NPB grown at 133 °C, showing full nucleation control at $p^* = 0.8$ (left) and partial nucleation control at $p^* = 1.3$ (right). Adapted with permission from ref 26. Copyright 2007 American Physical Society.

To gain deeper insight into the nucleation control mechanism, we conducted computer simulations by taking the SiO_2 substrate, Au dot, and deposited molecules as individual particles. A simple Lennard-Jones (L-J) pair potential was used to mimic the molecular interaction.[26,38−40] In the simulation, the number of molecule aggregates increases with the simulation time and saturates after a sufficient time. In analogy to experimental procedure, λ, p^*, and x_{NCE} were calculated and depicted as circles in Figure 5. The simulation results agree well with experimental results. The simulations are independent of microscopic details, indicating the generality of the physical mechanism.

The generality of the mechanism is further experimentally proven with different functional organic light-emitting molecules. By adjusting the dot array parameters, NPB, (dppy)BTPA, and DtCDQA can be deposited on predefined Au patterns on SiO_2 with full nucleation site control. Figure 6 shows blue, green, and orange light emission from uniform structure of the molecules.

The concept can be further used to create heteropatterns in which structures differ in thickness. Assuming that the uptake amount of evaporated molecules is independent of pattern size, then the height of the organic structures should be different: high on small patterns and low on big ones.

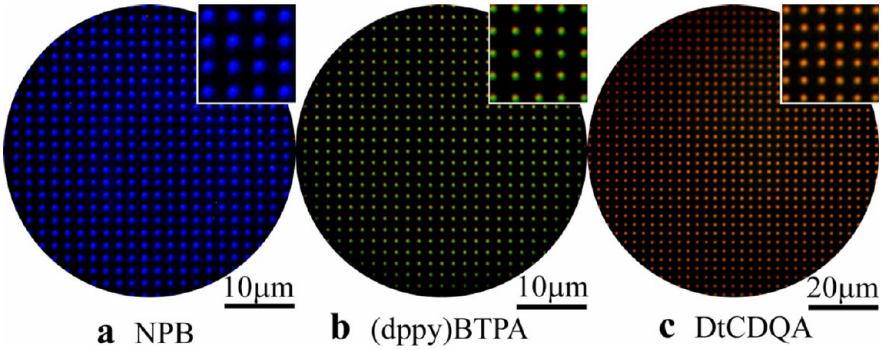

FIGURE 6. Fluorescent microscopy images of light-emitting organic patterns: (a) NPB (blue), $d = 600$ nm, $p = 1.8$ μm; (b) (dppy)BTPA (green), $d = 600$ nm, $p = 1.6$ μm; (c) DtCDQA (orange), $d = 1.0$ μm, $p = 2.5$ μm. The deposition rate and growth temperature for NPB, (dppy)BTPA, and DtCDQA are 0.1 nm/min and 133 °C, 0.1 nm/min and 129 °C, and 0.2 nm/min and 184 °C, respectively.

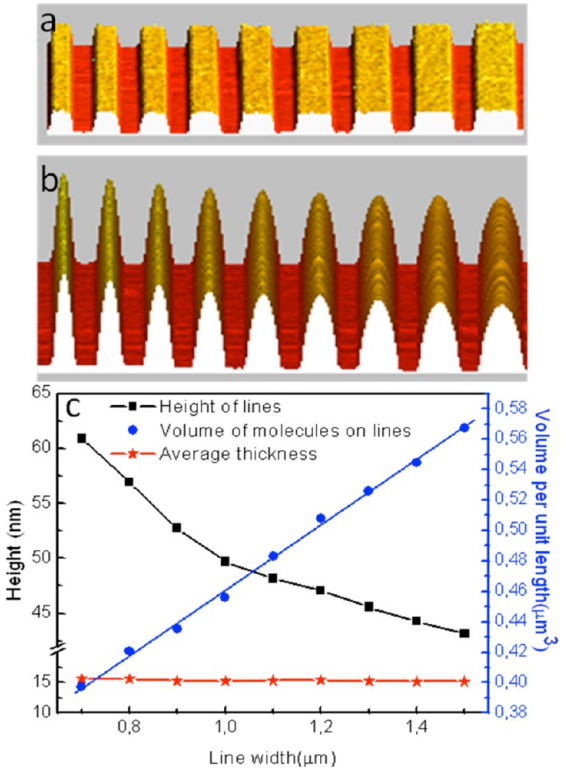

FIGURE 7. (a)Three-dimensional AFM image of Au lines with width increasing from 700 nm (left) to 1.5 μm (right) and spacing of 1 μm. (b) NPB lines formed on predefined Au lines. (c) Height, volume of molecules on each line, and average thickness of deposited molecules.

We proved the idea by using line shaped prepatterns with different width, as shown in Figure 7a. Figure 7b shows the height of lines, which varies with the line width. Figure 7c summarizes the height and the volume of lines as well as the average thickness of deposited molecules. The height of lines decreases as the line width increases (black squares). The volume of molecules on each line increases linearly with the line width (blue dots). By dividing the volume of molecules to effective area A ($A = (W + S)L$), where W is line width, S is the spacing between the lines, and L is the length of lines measured by AFM, we get the average thickness of molecules, which is determined by growth rate and time (red stars). This indicates that, by well designing the area ratio of prepattern and space, we can control the local thickness with very high resolution.

Step Edge Induced Area Selective Growth. Although there is a big selection of molecules that preferably form nuclei on Au areas instead of SiO_2 surface, not all molecules will behave in the same way. For instance, PTCDI-C_8 provides an exception. Both X-ray diffraction and AFM measurements on PTCDI-C_8 films grown on a SiO_2 surface at elevated substrate temperature indicate that the films

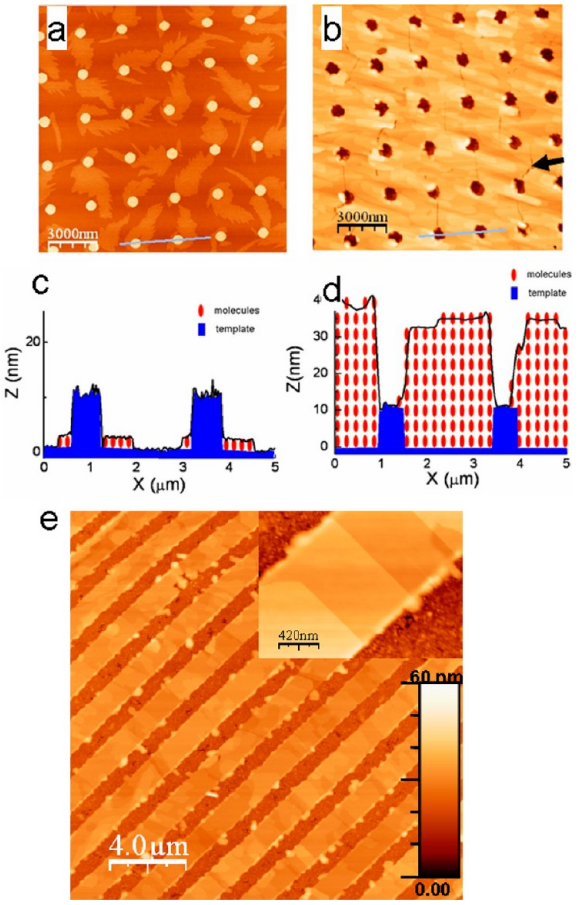

FIGURE 8. Topographic AFM images of PTCDI-C_8 grown on SiO_2 patterned with SiO_2 dots with a coverage of (a) 0.5 ML and (b) 20 ML. (c, d) Schematic representations of the building of topographic features together with measured topographic profiles marked by lines in panels a and b). (e) Topographic AFM images of PTCDI-C_8 grown on SiO_2 with Au lines. Inset shows a magnified view. Adapted with permission from ref 32. Copyright 2009 Wiley-VCH Verlag GmbH.

contain excellent *in* and *out* of plane molecular ordering, with the long axis of the perylene diimide core roughly parallel to the substrate normal.[32]

The surface morphology evolution of PTCDI-C_8 grown on a patterned substrate is shown in Figure 8. To clarify whether the nucleation is induced by binding energy difference or by the step edges of the patterns, we used SiO_2 instead of a Au dot array to pattern the SiO_2 surface. At low surface coverage (0.5 ML), monolayer PTCDI-C_8 domains that grow around the prepatterned SiO_2 dots were observed (Figure 8a). The growth is analogous to lateral epitaxy, which has been widely used to obtain high-quality GaN films.[41] Interestingly, with further deposition, no significant growth of PTCDI-C_8 layers took place on the SiO_2 dots, even when the thickness of the film exceeded the height of SiO_2 dots, as shown in Figure 8b. Based on the experimental results, a mechanism

for the selective growth was proposed as shown in Figure 8c,d. At the initial growth stage, deposited molecules move over the surface and search for the sites for nucleation. The edges of the pattern provide preferential sites for nucleation, similar to nucleation at atomic step edges.[35] The molecules will attach to the pattern edge by standing up-right, providing new nucleation sites for the subsequent molecules from diffusion or deposition, leading to lateral growth due to strong $\pi-\pi$ stacking and forming 2D terraces (Figure 8c). When the film thickness exceeds the height of the template, the molecules can still diffuse to PTCDI-C_8 area, probably owing to the difference of roughness in the two locations as shown in Figure 8c,d measured from AFM image profiles. The template surface (here CVD deposited SiO_2) is rougher than that of PTCDI-C_8 film, which might reduce the interaction between molecules and is unfavorable for film growth. The growth behavior is the same when using Au patterns. In this case, we can grow PTCDI-C_8 between Au lines on patterned SiO_2, resulting in crystalline PTCDI-C_8 films on SiO_2 with connection to the Au lines (Figure 8e). Such a configuration may find potential applications in OFETs with high-level integration.

Physical Property Tuning Based on Area-Selective Growth

Based on the principle of area-selective nucleation and growth demonstrated above, we are able to grow organic structures with tunable physical properties and fabricate devices with improved performances.

Tunable Single-, Double-, and Triple-Color Patterns with Two Compounds. OLEDs have attracted intensive attention for applications like lighting, displays, and sensors. Color integration on a single substrate is critical for products like full color displays. Mostly, the challenge lies in the production of user-defined multicolor patterns owing to the absence of patterning techniques. Usually, colored patterns are composed of different molecules with different emissions. However, realization of multicolor emission on predefined locations with fewer compounds is of great advantage in simplifying both fabrication and characterization of devices.

Here we show that tunable single-, double- and triple-color patterns can be simply realized by extending the nucleation control strategy to more than one kind of molecule.[30,42] Figure 9a schematically shows the evolution of patterned growth with two kinds of molecules. For example, NPB and DtCDQA were deposited simultaneously on a Au dot array patterned SiO_2 surface with different mixing ratio. AFM measurements show that both molecules can selectively nucleate on a predefined Au area with optimization of *T*, *F*, and *p*, as one example shown in Figure 9b with a mixing ratio of 9:1 (NPB/DtCDQA). More importantly, the mixing ratio of DtCDQA and NPB strongly influences the emission color of the organic nuclei (Figure 9c).

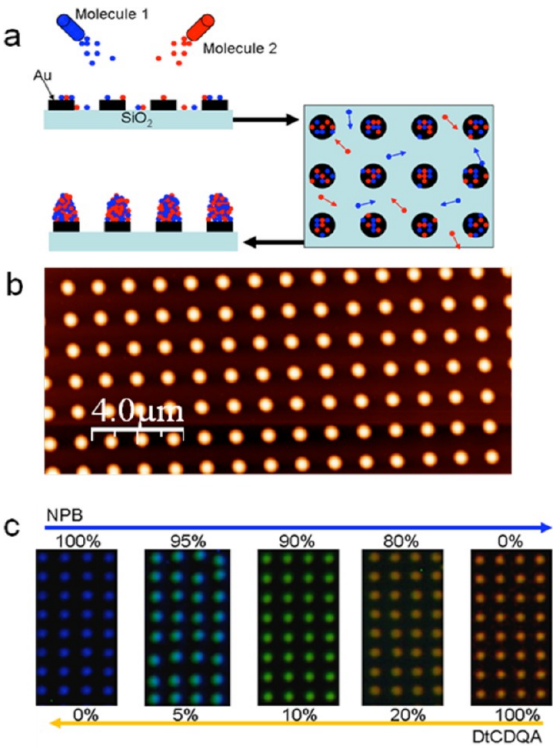

FIGURE 9. (a) Schematic evolution of patterned growth with two molecules on a patterned substrate. The molecules, sublimed from a crucible and deposited on the substrate (top left, side view), can diffuse over the surface (right, top view) and prefer to nucleate on the pre-patterned Au positions (left bottom, side view). (b) Morphology of the co-deposited NPB and DtCDQA (mixing ratio of 9:1). (c) Fluorescence microscopy image of co-deposited NPB and DtCDQA with different mixing ratio. Adapted with permission from ref 30. Copyright 2010 Wiley-VCH Verlag GmbH.

Photoluminescence (PL) measurements were performed to investigate the origin of the color tuning with two kinds of dye molecules. PL spectra from pure NPB and DtCDQA patterns (black lines in Figure 10a,b, respectively) show the emissions of NPB at 460 nm and DtCDQA at 583 nm, which are similar to their powder states. The co-deposited samples exhibit DtCDQA concentration-dependent PL (Figure 10a,b). Besides the NPB emission (I_{NPB}), the co-deposited samples also contain emissions centered at 527 and 557 nm from DtCDQA monomer (I_{DM}) and aggregate (I_{DA}), respectively at low concentration of less than 20%. At the high concentration of more than 33%, the spectra are dominated by DtCDQA aggregate emission. The relative intensity ratios

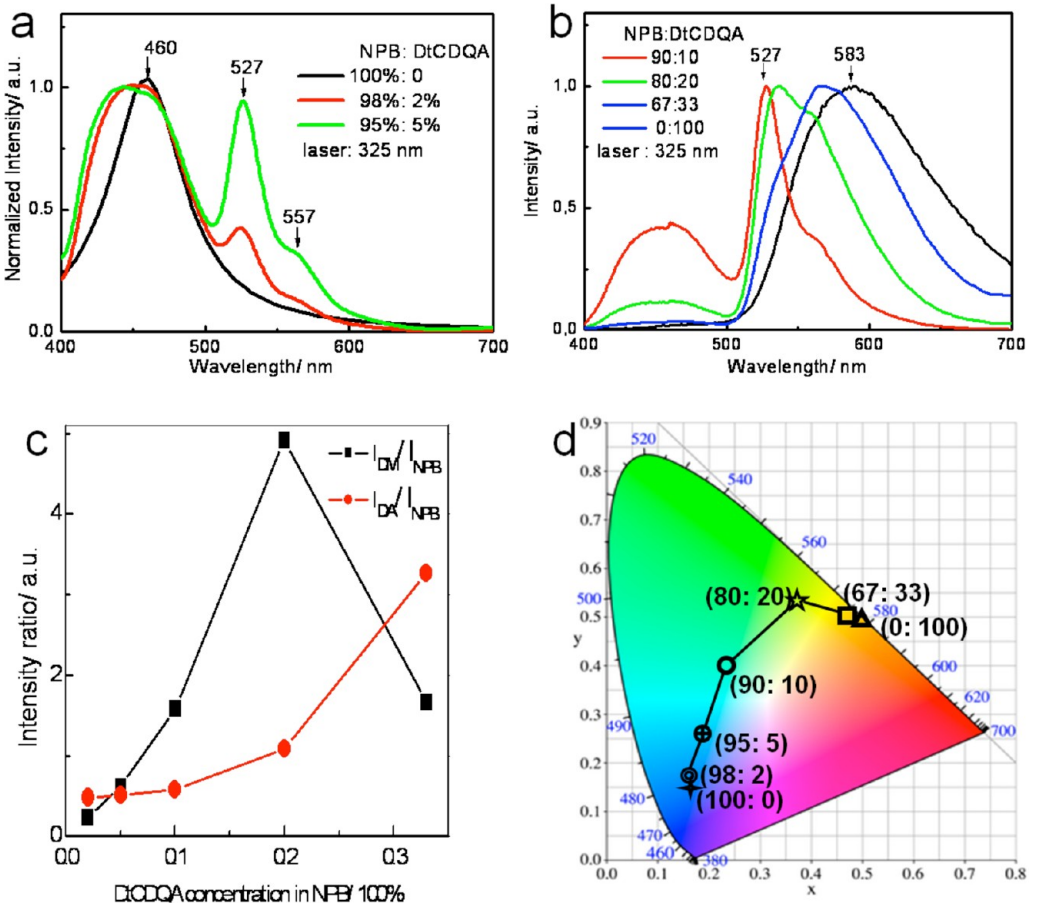

FIGURE 10. (a, b) PL spectra of NPB and DtCDQA co-deposited on a patterned substrate. (c) Relative intensity of DtCDQA monomer emission (I_{DM}) and aggregate emission (I_{DA}) to NPB emission (I_{NPB}) with different mixing ratios. (d) CIE chromaticity diagram showing chromaticity coordinates of PL spectra in panels a and b. The numbers in brackets are the mixing ratio of the two molecules. Adapted with permission from ref 30. Copyright 2010 Wiley-VCH Verlag GmbH.

of the emissions vary with the mixing ratios of the two compounds, as shown in Figure 10c. Replotting of Figure 10a,b on the calculated 1931 Commission Internationle de L'Eclairage (*x*, *y*) coordinates (CIE*x*, *y*) shows that a PL color tuning from blue to green and then to orange can clearly be traced, shown in Figure 10d.

The dependence of PL on DtCDQA concentration in NPB enables us to further fabricate tunable bicolor patterns. A key point here is to create DtCDQA patterns with different thickness at predefined areas. Such patterns can be realized by two-step growth at different substrate temperatures, as schematically shown in Figure 11a. DtCDQA molecules were first grown at high temperature to nucleate on Au and then at reduced temperature to cover the whole substrate surface, creating a molecule thickness of h_1 on Au and h_2 on SiO_2. Taking the Au line array (width of 1 μm and periodicity of 5 μm) patterned SiO_2 as an example, we achieved h_1 of 32 nm and h_2 of 1 nm by deposition of 5 nm DtCDQA at 180 °C followed by 1 nm at 50 °C, as shown in Figure 11b. With small volume of NPB deposition at optimized substrate temperature, the DtCDQA aggregate emission (thick film) dominates on Au and monomer emission (thin film) on SiO_2, leading to the orange–green bicolor pattern as shown in Figure 11c. Furthermore, the colored patterns can be tuned to blue–green ones by further deposition of 100 nm NPB, shown in Figure 11d. The additional deposited NPB dilutes DtCDQA on the Au area forming monomers, leading to emission of green light. While on the SiO_2 area, the concentration of DtCDQA is very low and NPB dominates the emission, which gives rise to a blue color. In this way, tunable bicolor patterns can be achieved with two kinds of molecules by simply adjusting the thickness of DtCDQA and NPB on the patterned surface.

Color-Tuning Based on Liquid-Behavior of Evaporated Molecules. Contrary to NPB deposited on Au stripes with different width on SiO_2 surface, where the height simply decreases with the increase of stripe width (Figure 7), DtCDQA on similarly prepatterned surface contains three

features, as shown in Figure 12a: molecule stripes on Au shaped as cylindrical segments, bulges positioned on both Au lines and SiO_2, and droplets shaped as spherical caps on bare SiO_2. The morphologies evolve from several states viewed by AFM with increasing amounts of deposited molecules: random droplets, elongated drops, and molecule lines on Au stripes, as well as bulges riding on both Au and SiO_2. AFM measurements further reveal that all three features obey linear relationships of height to width, shown in Figure 12b. Such a behavior is typically observed in liquids, for example, water on hydrophobic/hydrophilic patterned surfaces, implying that the molecular aggregates are in the liquid state on the surface at elevated temperature (e.g., 180 °C for DtCDQA).

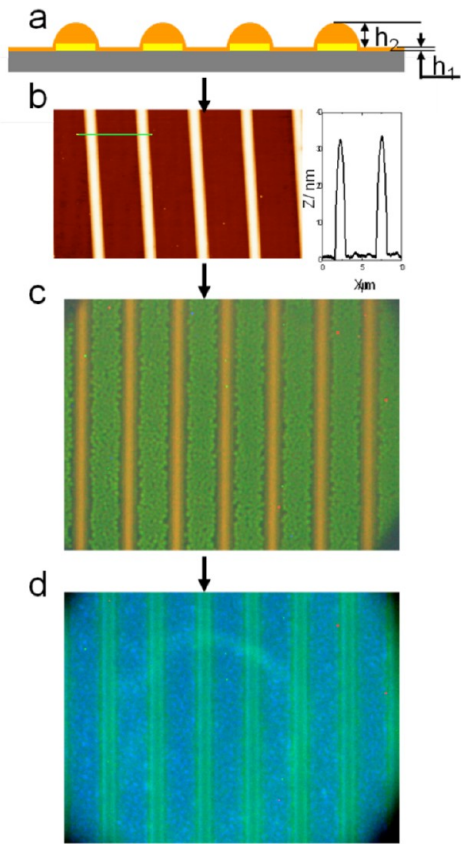

FIGURE 11. (a) Schematic representation of DtCDQA distribution on patterned surface by a two step growth technique. (b) left: AFM images of 5 nm DtCDQA grown at 180 °C followed by 1 nm DtCDQA at 50 °C on a Au line array patterned SiO_2, resulting h1 of 32 nm and h2 of 1 nm shown in AFM profile of right side. (c, d) Fluorescence microscopy images of 10 nm (c) and 100 nm (d) NPB deposited on samples shown in (b) at 100 °C.

Considering liquids on a stripe-patterned surface, the height of the liquid stripe is determined by a contact angle θ and stripe width w. In this case, heteropatterning with height varying with stripe width can also be achieved, similar to NPB on such patterns but with an inverse $h-w$ relationship. The w dependent h property enables us to fabricate triple color patterns with two kinds of molecules, by adopting DtCDQA concentration-dependent color tuning described above. However, the formation of bulges is a key problem to achieve a homogeneous multicolor pattern: Bulges are already formed on narrow Au stripes, while the wide ones are still not fully covered.[42] Owing to an energy barrier for the stripe evolving to bulges[43] and molecular diffusion over the surface at elevated substrate temperature, molecules can transfer from narrow Au stripes to wide ones via diffusion when the space between them is small enough, achieving high-resolution DtCDQA patterns with height difference on the predefined areas (Figure 13a). With the DtCDQA pattern presented in Figure 13a, which contains

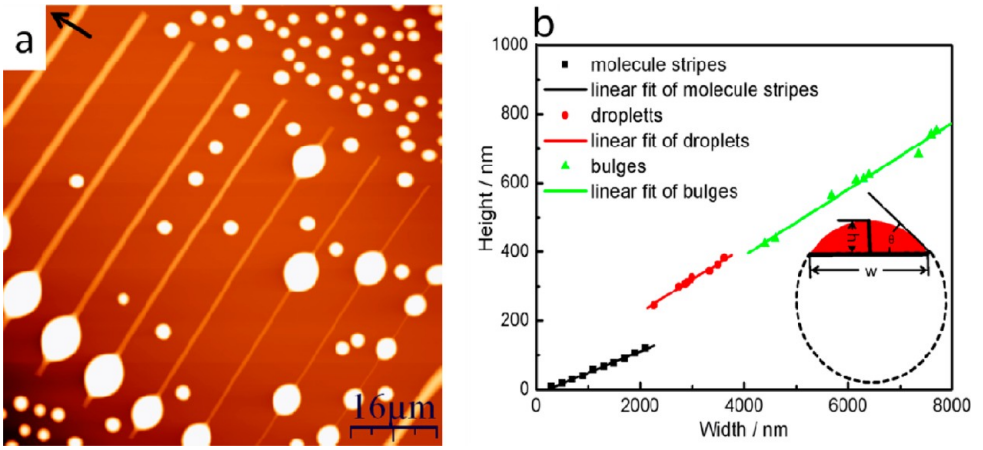

FIGURE 12. (a) AFM image of 50 nm DtCDQA grown on 10 Au line patterned SiO_2. The Au line widths vary from 0.3 to 2.3 μm with 0.2 μm increments. The DtCDQA molecules are present in three morphologies that are molecule stripe, bulge, and droplet with height–width relationship shown in panel b. The height and width are determined by taking cross section profiles of AFM images with direction indicated by an arrow in panel a. Adapted with permission from ref 42. Copyright 2011 Wiley-VCH Verlag GmbH.

uncovered SiO_2, 22 nm DtCDQA on the narrow Au stripes, and 120 nm DtCDQA on the wide Au stripes, we obtained the triple color pattern by simply depositing NPB molecules on the DtCDQA structured surface, as shown in Figure 13b. The three colors, blue, green, and orange, originate from NPB emission on uncovered SiO_2, DtCDQA monomer emission on narrow Au stripes, and DtCDQA aggregate emission on wide Au stripes. In principal, tunable multicolor (more than three) patterns can also be achieved by controlling the prepattern size and NPB amount.

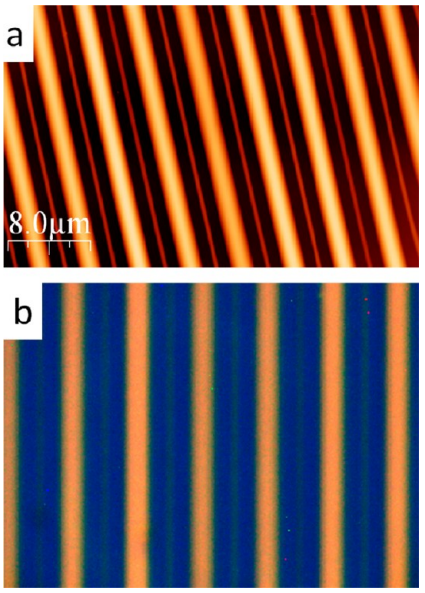

FIGURE 13. (a) AFM image of 30 nm DtCDQA grown on alternating 0.5 and 2 μm hierarchical Au lines patterned SiO_2 with spacing of 1 μm, and (b) Fluorescence microscopy image of 150 nm NPB deposited on DtCDQA heteropatterned surface in (a).

Molecule Separation at Mesotropic Scale. Combing the two growth modes, namely, binding energy difference induced growth and step edge-induced growth, molecular separation can be achieved on prepatterned surfaces. Taking a Au dot array patterned SiO_2 surface (Figure 14a) as an example, PTCDI-C_8 molecules are controlled to grow on the SiO_2 rather than on Au areas (Figure 14b). The upright orientation of PTCDI-C_8 leaves an inert alkyl surface, which enables NPB to move along the surface and nucleate on the Au areas, as shown in Figure 14c. The separation process is depicted schematically in Figure 14d.

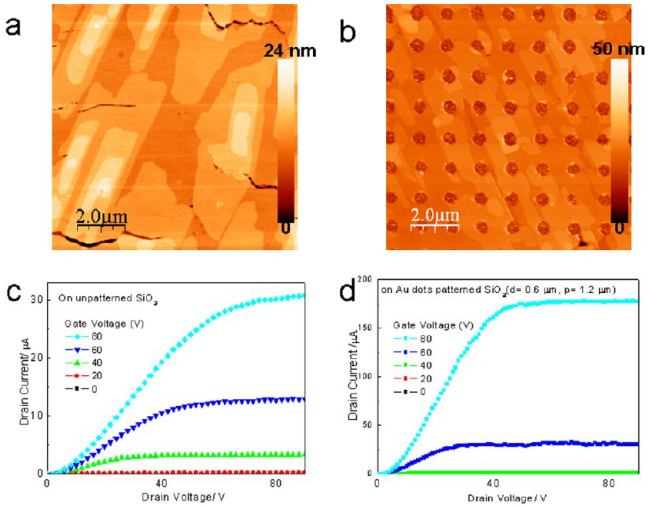

FIGURE 15. Morphology of bottom contact OFETs of PTCDI-C_8 films. Cooling to room temperature from a substrate temperature of 170 °C (a) on an unpatterned SiO_2 and (b) on a Au dot array ($h = 30$ nm, $d = 0.6$ μm, $p = 1.2$ μm) patterned SiO_2. (c, d) Output characteristics of the OFTEs shown in panels a and b. Adapted with permission from ref 32. Copyright 2009 Wiley-VCH Verlag GmbH.

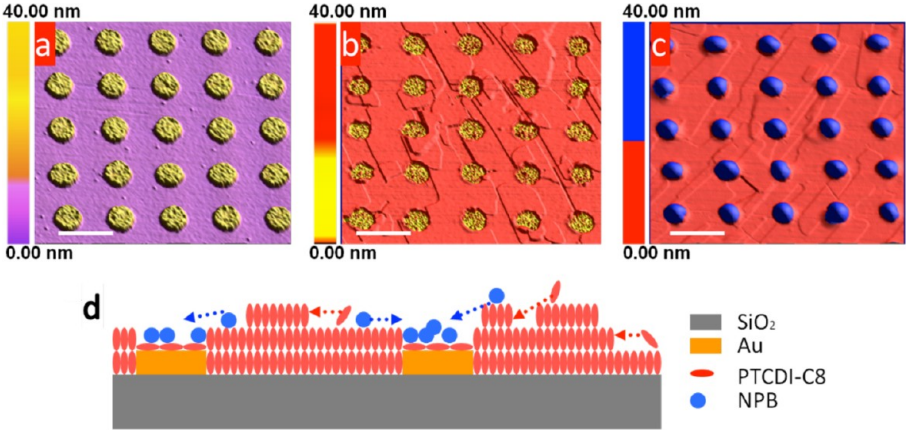

FIGURE 14. Three-dimensional morphology evolution viewed by AFM and schematic representation of separating molecules by nucleation site recognition: (a) SiO_2 patterned with an array of Au dots; (b) upon deposition of 10 nm of PTCDI-C_8 on the patterned SiO_2 layer; (c) further deposition of 3 nm of NPB on the sample shown in panel b; (d) schematic representation of the deposition. The scale bars in panels a–c are 1.2 μm.

OFETs with Improved Mobility. Organic films with large crystalline domains and few defects are key issues for organic semiconductor devices, especially for high-performance OFETs. However, such films are normally grown at high substrate temperature, which will crack while cooling for device processing owing to thermal mismatch.[44] Figure 15a shows such cracks in PTCDI-C_8 grown on a flat SiO_2 at high substrate temperature. For PTCDI-C_8 grown on a patterned substrate, such cracks can be effectively suppressed by optimizing template dimensions, as shown in Figure 15b. The elimination of the cracks can be attributed to the presence of interfaces between the organic film and predefined inorganic pattern, which act as strain relief areas.[45]

Bottom contact FETs, on both cracked and uncraked films with morphologies shown in Figure 15a,b, were further fabricated to evaluate the film quality. The output characteristics of FETs on both the cracked and uncracked films are shown in Figure 15c,d, yielding electron mobility in the saturation region of 0.13 and 1.0 $cm^2\ V^{-1}\ s^{-1}$, respectively. Both the morphology and electrical properties indicate that patterned growth provides a simple and efficient way to obtain high-quality, crack-free films.

Conclusions and Outlook

Over the last two decades, exciting progress in many aspects of organic semiconductors has been witnessed, and the pace of the progress has continued to accelerate. Patterning of functional organic molecules with high resolution and high yield over large areas is enormously challenging. We proposed a concept to turn over the "film growth and then patterning" to "prepatterning and then selective nucleation and growth". On this basis, two different selective growth mechanisms are observed. The method can be applied to different kinds of molecules to realize functional molecular architectures and improve device performance. We believe the methods represent essential steps toward practical applications of organic semiconductor devices with high level of integration.

Considerable work is still required to turn these techniques into a truly viable technology. A key advantage of the organic semiconductor lies on their potential low cost over a large area. In combination with parallel patterning techniques like photolithography, the nucleation control strategy will make an efficient way to generate organic patterns. Till now, work was done on Si wafers with thermal oxides. Transferring the technique to cheap substrates such as glass and flexible materials is an essential step for success.

In organic microelectronics, applications such as electronic paper and RFID are the most promising applications suitable for the organic semiconductors. To achieve this, addressable, cross-talk free, and high-level integration device processing technology is additionally required. With the concept we proposed and the proof of principle we demonstrated, it is possible to develop a general lithography compatible method to fabricate organic electronic devices with reduced size and high integration level, which in return reduce fabrication cost per device.

This work was supported through the Transregional Collaborative Research Centre TRR 61 by the DFG, and FP7-PEOPLE-2009-IRSES/247641.

BIOGRAPHICAL INFORMATION

Wenchong Wang obtained his B.S. degree from Xi'an Jiaotong University, China, in 1998. He received his Ph.D. degree from Institute of Physics, Chinese Academy of Sciences, China, in 2003, working on Molecular Beam Epitaxy. He was a research scientist at Madrid Microelectronics Institute, National Centre for Microelectronics, Spain. He is presently a research fellow at Institute of Physics, Münster University, and CeNTech, Germany. He is developing a photolithography compatible technique to pattern organic semiconductors and is currently interested in applications of the technique to organic and organic/inorganic hybrid electronics.

Lifeng Chi received her B.S. degree in physics and M.S. degree in physical chemistry at Jilin University, China. She earned her Ph.D. degree in 1989 in Göttingen, Germany, working on electron/energy transfer in thin organic films. After a postdoctoral stay at the University of Mainz and BASF, she moved to University of Münster and received a Lise Meitner scholarship in 1997. In 2000, she finished her habilitation in physics working on nanostructuring through self-organization. She became a professor in physics at the University of Münster in 2004. Her research interests include surface (nano)patterning, molecular self-assembly on structured surfaces, low-dimensional molecular electronics, and on-surface chemistry. She has coauthored ca. 230 original scientific papers, coauthored 4 books and edited one book, and filed 10 patents.

FOOTNOTES

*To whom correspondence should be addressed. E-mail: chi@uni-muenster.de.
The authors declare no competing financial interest.

REFERENCES

1 Forrest, S. R. The path to ubiquitous and low-cost organic electronic appliances on plastic. *Nature* **2004**, *428*, 911–918.
2 Horowitz, G. Organic thin film transistors: From theory to real devices. *J. Mater. Res.* **2004**, *19*, 1946–1962.
3 Kippelen, B.; Brédas, J. L. Organic photovoltaics. *Energy Environ. Sci.* **2009**, *2*, 251–261.
4 Bao, Z.; Lovinger, A. J.; Brown, J. New air-stable n-channel organic thin film transistors. *J. Am. Chem. Soc.* **1998**, *120*, 207–208.
5 Jackel, F.; Watson, M. D.; Mullen, K.; Rabe, J. P. Prototypical single-molecule chemical-field-effect transistor with nanometer-sized gates. *Phys. Rev. Lett.* **2004**, *92*, No. 188303.

6 Mas-Torrent, M.; Rovira, C. Novel small molecules for organic field-effect transistors: Towards processability and high performance. *Chem. Soc. Rev.* **2008**, *37*, 827–838.

7 Briseno, A. L.; Mannsfeld, S. C. B.; Ling, M. M.; Liu, S. H.; Tseng, R. J.; Reese, C.; Roberts, M. E.; Yang, Y.; Wudl, F.; Bao, Z. N. Patterning organic single-crystal transistor arrays. *Nature* **2006**, *444*, 913–917.

8 Minemawari, H.; Yamada, T.; Matsui, H.; Tsutsumi, J.; Haas, S.; Chiba, R.; Kumai, R.; Hasegawa, T. Inkjet printing of single-crystal films. *Nature* **2011**, *475*, 364–367.

9 Holder, E.; Langeveld, B. M. W.; Schbert, U. S. New trends in the use of transition metal-ligand complexes for applications in electroluminescent devices. *Adv. Mater.* **2005**, *9*, 1109–1121.

10 Walzer, K.; Maennig, B.; Pfeiffer, M.; Leo, K. Highly efficient organic devices based on electrically doped transport. *Chem. Rev.* **2007**, *107*, 1233–1271.

11 Bredas, J. L.; Norton, J.; Cornil, J.; Coropceanu, V. Molecular understanding of organic solar cells: The challenges. *Acc. Chem. Res.* **2009**, *42*, 1691–1699.

12 Reed, M. A.; Chen, J.; Rawlett, A. M.; Price, D. W.; Tour, J. M. Molecular random access memory cell. *Appl. Phys. Lett.* **2001**, *78*, 3735–3737.

13 Guo, Y.; Yu, G.; Liu, Y. Functional organic field-effect transistors. *Adv. Mater.* **2010**, *22*, 4427–4447.

14 So, F.; Kondakov, D. Degradation mechanisms in small-molecule and polymer organic light-emitting diodes. *Adv. Mater.* **2010**, *22*, 3762–3777.

15 Tian, P. F.; Bulovic, V.; Burrows, P. E.; Gu, G.; Forrest, S. R.; Zhou, T. X. Precise, scalable shadow mask patterning of vacuum-deposited organic light emitting devices. *J. Vac. Sci. Technol. B* **1999**, *17*, 2975–2981.

16 Kim, C.; Burrows, P. E.; Forrest, S. R. Micropatterning of organic electronic devices by cold-welding. *Science* **2000**, *288*, 831–833.

17 Sirringhaus, H.; Kawase, T.; Friend, R. H.; Shimoda, T.; Inbasekaran, M.; Wu, W.; Woo, E. P. High-resolution inkjet printing of all-polymer transistor circuits. *Science* **2000**, *290*, 2123–2126.

18 Shtein, M.; Peumans, P.; Benziger, J. B.; Forrest, S. R. Direct, mask- and solvent-free printing of molecular organic semiconductors. *Adv. Mater.* **2004**, *16*, 1615–1620.

19 Wang, J. Z.; Zheng, Z. H.; Li, H. W.; Huck, W. T. S.; Sirringhaus, H. Dewetting of conducting polymer inkjet droplets on patterned surfaces. *Nat. Mater.* **2004**, *3*, 171–176.

20 Tian, P. F.; Burrows, P. E.; Forrest, S. R. Photolithographic patterning of vacuum-deposited organic light emitting devices. *Appl. Phys. Lett.* **1997**, *71*, 3197–3199.

21 Kymissis, I.; Dimitrakopoulos, C. D.; Purushothaman, S. Patterning pentacene organic thin film transistors. *J. Vac. Sci. Technol. B* **2002**, *20*, 956–959.

22 Barth, J. V.; Costantini, G.; Kern, K. Engineering atomic and molecular nanostructures at surfaces. *Nature* **2005**, *437*, 671–679.

23 Henzie, J.; Barton, J. E.; Stender, C. L.; Odom, T. W. Large-area nanoscale patterning: Chemistry meets fabrication. *Acc. Chem. Res.* **2006**, *39*, 249–257.

24 Aizenberg, J.; Black, A. J.; Whitesides, G. M. Control of crystal nucleation by patterned self-assembled monolayers. *Nature* **1999**, *398*, 495–498.

25 Mendez, J.; Caillard, R.; Otero, G.; Nicoara, N.; Martin-Gago, J. A. Nanostructured organic material: From molecular chains to organic nanodots. *Adv. Mater.* **2006**, *18*, 2048–2052.

26 Wang, W. C.; Zhong, D. Y.; Zhu, J.; Kalischewski, F.; Dou, R. F.; Wedeking, K.; Wang, Y.; Heuer, A.; Fuchs, H.; Erker, G.; Chi, L. F. Patterned nucleation control in vacuum deposition of organic molecules. *Phys. Rev. Lett.* **2007**, *98*, No. 225504.

27 Wedeking, K.; Mu, Z. C.; Kehr, G.; Sierra, J. C.; Lichtenfeld, C. M.; Grimme, S.; Erker, G.; Frohlich, R.; Chi, L. F.; Wang, W. C.; Zhong, D. Y.; Fuchs, H. Oligoethylene chains terminated by ferrocenyl end groups: Synthesis, structural properties, and two-dimensional self-assembly on surfaces. *Chem.—Eur. J.* **2006**, *12*, 1618–1628.

28 Tang, C. W.; Vanslyke, S. A. Organic electroluminescent diodes. *Appl. Phys. Lett.* **1987**, *51*, 913–915.

29 Zhang, H. Y.; Huo, C.; Zhang, J. Y.; Zhang, P.; Tian, W. J.; Wang, Y. Efficient single-layer electroluminescent device based on a bipolar emitting boron-containing material. *Chem. Commun.* **2006**, *3*, 281–283.

30 Wang, W. C.; Du, C.; Bi, H.; Wang, Y.; Mauser, C.; Da Como, E.; Fuchs, H.; Chi, L. F. Tunable multicolor ordered patterns with two dye molecules. *Adv. Mater.* **2010**, *22*, 2764–2769.

31 Malenfant, P. R. L.; Dimitrakopoulos, C. D.; Gelorme, J. D.; Kosbar, L. L.; Graham, T. O.; Curioni, A.; Andreoni, W. N-type organic thin-film transistor with high field-effect mobility based on a N,N′-dialkyl-3,4,9,10-perylene tetracarboxylic diimide derivative. *Appl. Phys. Lett.* **2002**, *80*, 2517–2519.

32 Wang, W. C.; Du, C.; Zhong, D. Y.; Hirtz, M.; Wang, Y.; Lu, N.; Wu, L. X.; Ebeling, D.; Li, L. Q.; Fuchs, H.; Chi, L. F. Control over patterning of organic semiconductors: step-edge-induced area selective growth. *Adv. Mater.* **2009**, *21*, 4721–4725.

33 Heringdorf, F. J. M. Z.; Reuter, M. C.; Tromp, R. M. Growth dynamics of pentacene thin films. *Nature* **2001**, *412*, 517–520.

34 Florez, E.; Mondragon, F.; Truong, T. N.; Fuentealba, P. Density functional theory characterization of the formation of copper clusters on F-s and F-s(+) centers on a MgO surface. *Surf. Sci.* **2007**, *601*, 656–664.

35 Bohringer, M.; Morgenstern, K.; Schneider, W. D.; Wuhn, M.; Woll, C.; Berndt, R. Self-assembly of 1-nitronaphthalene on Au(111). *Surf. Sci.* **2000**, *444*, 199–210.

36 Mendez, J.; Caillard, R.; Otero, G.; Nicoara, N.; Martin-Gago, J. A. Nanostructured organic material: From molecular chains to organic nanodots. *Adv. Mater.* **2006**, *18*, 2048–2052.

37 Wang, L. G.; Kratzer, P.; Scheffler, M.; Moll, N. Formation and stability of self-assembled coherent islands in highly mismatched heteroepitaxy. *Phys. Rev. Lett.* **1999**, *82*, 4042–4045.

38 Kalischewski, F.; Zhu, J.; Heuer, A. Loss of control in pattern-directed nucleation: A theoretical study. *Phys. Rev. B* **2008**, *78*, No. 155401.

39 Kalischewski, F.; Herer, A. Dynamic effects on the loss of control in template-directed nucleation. *Phys. Rev. B.* **2009**, *80*, No. 155421.

40 Lied, F.; Mues, T.; Wang, W. C.; Chi, L. F.; Heuer, A. Different growth regimes on prepatterned surfaces: Consistent evidence from simulations and experiments. *J. Chem. Phys.* **2012**, *136*, No. 024704.

41 Beaumont, B.; Vennegues, P.; Gibart, P. Epitaxial lateral overgrowth of GaN, Phys. *Status Solidi B* **2001**, *227*, 1–43.

42 Wang, W. C.; Du, C.; Wang, C. G.; Hirtz, H.; Li, L. Q.; Hao, J. Y.; Wu, Q.; Lu, R.; Lu, N.; Wang, Y.; Fuchs, H.; Chi, L. F. High-resolution triple-color patterns based on the liquid behavior of organic molecules. *Small* **2011**, *7*, 1403–1406.

43 Valencia, A.; Lipowsky, R. Nucleation through a double barrier on a chemically patterned substrate. *Langmuir* **2004**, *20*, 1986–1996.

44 Tatemichi, S.; Ichikawa, M.; Koyama, T.; Taniguchi, Y. High mobility n-type thin-film transistors based on N,N′-ditridecyl perylene diimide with thermal treatments. *Appl. Phys. Lett.* **2006**, *89*, No. 112108.

45 Krost, A.; Dadgar, A. GaN-based optoelectronics on silicon substrates. *Mater. Sci. Eng., B* **2002**, *93*, 77–84.